Electronic Supplementary Material (ESI) for Soft Matter.

Supporting Information
Gelation under stress: impact of shear flow on the formation and mechanical properties of methylcellulose hydrogels

Arif Z. Nelson[1], Yilin Wang[1], Yushi Wang[1], Anthony S. Margotta[1], Robert L. Sammler[2], Aslin Izmitli[3], Joshua S. Katz[3], Jaime Curtis-Fisk[4], Yongfu Li[5], Randy H. Ewoldt[1]*

[1]Department of Mechanical Science and Engineering, University of Illinois at Urbana-Champaign, Urbana, IL 61801, USA

[2]Formulation, Automation, and Material Science and Engineering, Corporate R&D, Dow Inc., Midland, MI 48674, USA

[3]Home and Personal Care TS&D, Dow Inc., Collegeville, PA 19426, USA

[4]Pharma Solutions R&D, International Flavors & Fragrances, Wilmington, DE 19803, USA

[5]Analytical Science, Corporate R&D, Dow Inc., Midland, MI 48674, USA

I. Application Stress Magnitudes

This section demonstrates the calculations of representative stress magnitudes relevant for several application scenarios. In all of these scenarios, we will assume a density of water for the material (ρ = 1000 kg.m^{-3}). Naturally, methylcellulose solutions have a density slightly greater than water, but this is insignificant for the estimates here.

Gravitational stress on a vertical surface. Given a uniform layer shown in Figure S1A, with free-body diagram shown in Figure S1B, the maximum stress, σ, distributed over the contact area, bc, is balanced by the weight of the layer, W.

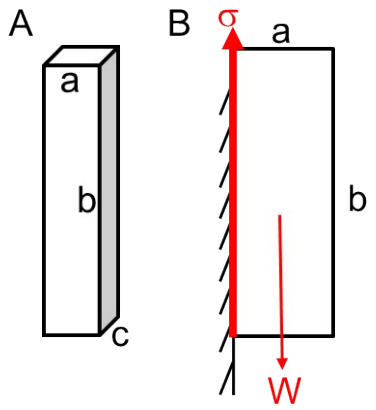

Figure S1. A) Uniform layer with B) free-body diagram. Maximum shear stress occurs at the wall contact

Assuming uniform density, for a given maximum stress, $\sigma_{\max}$, balancing the forces and solving for the maximum thickness results in

$$a_{\max} = \frac{\sigma_{\max}}{\rho g} \ , \qquad \text{* MERGEFORMAT (1)}$$

where g is the gravitational constant. More specifically, we can approximate the maximum gravitational stress of a layer of thickness, *a*, with density of water on a vertical surface with Earth gravitational constant as

$$\sigma_{\max} \approx \left(10^4 \frac{\mathrm{N}}{\mathrm{m}^3}\right) a \ . \qquad \text{* MERGEFORMAT (2)}$$

For example, a 1mm thick coating experiences a maximum stress $\sigma_{\max} \approx 10\ \mathrm{Pa}$, as indicated in Figure 2 in the main paper.

Characteristic stress of droplet impact. Given a spherical drop of diameter D, impacting a surface at a velocity v, we can develop a scaling law that relates a

characteristic impact stress to the velocity of the droplet. Using the work-energy theorem, where the change in kinetic energy is equal to the work done on the droplet, we can represent the work done as,

$$\sigma\left(\text{Area}\right)\left(\text{Distance}\right) \sim \sigma\left(D^2\right)\left(D\right), \qquad \text{* MERGEFORMAT (3)}$$

which we set equal to the change in kinetic energy for the droplet to come to rest,

$$\frac{1}{2}mv^2 = \frac{1}{2}\rho V v^2 \qquad \text{* MERGEFORMAT (4)}$$

where V is the volume of the droplet which is proportional to D^3, and ρ is the density which we will approximate as that of water. Solving for the characteristic stress provides an estimate of stress that is consistent with the dynamic pressure to stagnate fluid flow,

$$\begin{aligned} \sigma &\sim \rho v^2 \\ &\approx \left(10^3 \frac{\text{kg}}{\text{m}^3}\right) v^2 \end{aligned} \qquad \text{* MERGEFORMAT (5)}$$

Droplet velocities during spray coating can vary over a wide range. Perhaps on the slower end, consider a velocity of 0.3 m/s, which relates to characteristics stresses at impact of almost 100 Pa, as indicated in Figure 2 of the main text.

Characteristic stress of particle settling. A gelled sample could inhibit particle sedimentation (or rising of air bubbles), but only if gelation can still occur under the associated dynamic stress conditions. Given a particle of diameter D, with a density difference comparable to the density of the surrounding medium ($\Delta\rho = \rho$, e.g. for an air bubble, or a particle at twice the density of the liquid), the characteristic stress scales as,

$$\sigma \sim \frac{\text{Net Weight/Buoyant Force}}{\text{Area}} \sim \frac{\rho g D^3}{D^2} \quad . \qquad \text{* MERGEFORMAT (6)}$$

Thus, for density differences on the order of water, and surface gravitational strength, the characteristic stress is estimated by

$$\sigma \approx \left(10^4 \frac{\mathrm{N}}{\mathrm{m}^3}\right) D . \qquad \text{* MERGEFORMAT (7)}$$

For example, 1 mm diameter particles are associated with stresses on the order of 10 Pa, easily enough to disrupt gel formation for the formulations considered in this work.

II. Full Rheological Data

Quiescent gel point. Figures S2 through S6 show the small amplitude oscillatory shear (SAOS) measurements performed using the protocol detailed in the Experimental Section for all tested concentrations not shown in the main work. The “0 Pa” gel temperature for each concentration was determined from the crossover of G' and G'', except for 2.08 wt%, the gel temperature of which was determined from the maximum slope of the moduli. Sub-dominant modulus data past the gel point was often difficult to resolve, particularly at higher concentrations; regions with non-physical moduli (i.e. negative values) are omitted for clarity. All error bars are from three repeat measurements; error bars not shown are smaller than the data points.

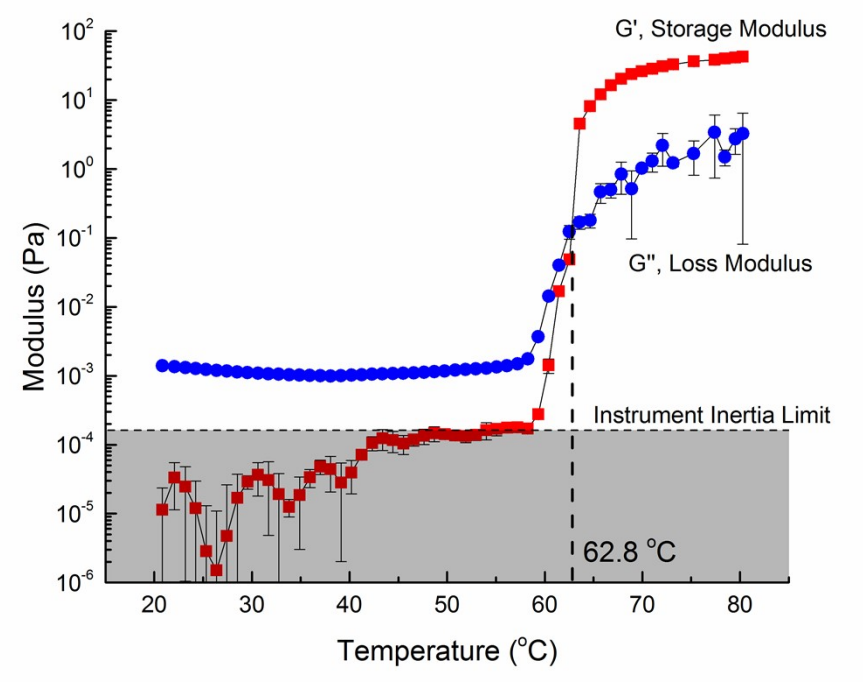

Figure S2. G' and G'' from SAOS measurements for MC 1.04 wt% (oscillation frequency = 0.1 rad/s, stress amplitude = 0.1 Pa) while warming from 20 to 80 °C at 1 °C/min.

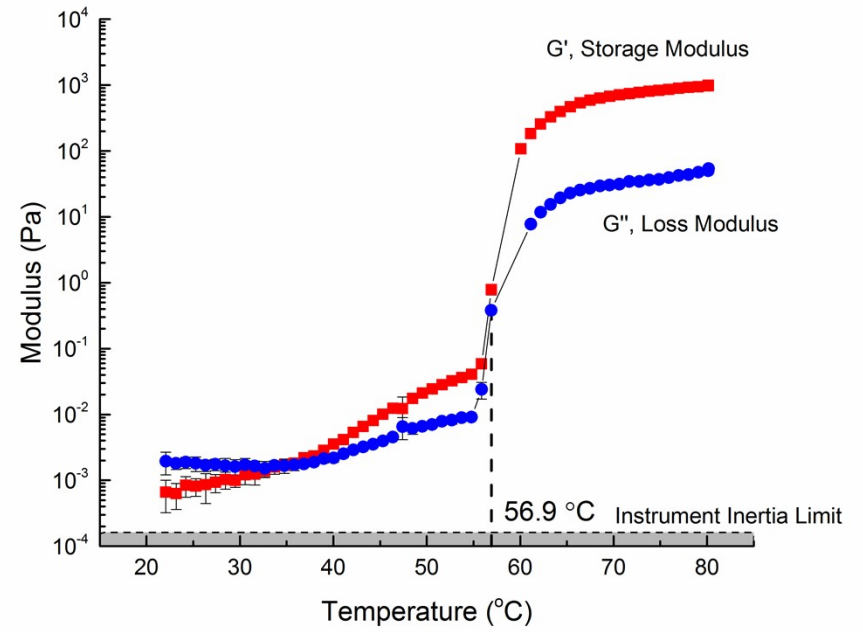

Figure S3. G' and G'' from SAOS measurements for MC 2.08 wt% (oscillation frequency = 0.1 rad/s, stress amplitude = 0.1 Pa) while warming from 20 to 80 °C at 1 °C/min. Gel temperature was determined from the maximum slope of the moduli.

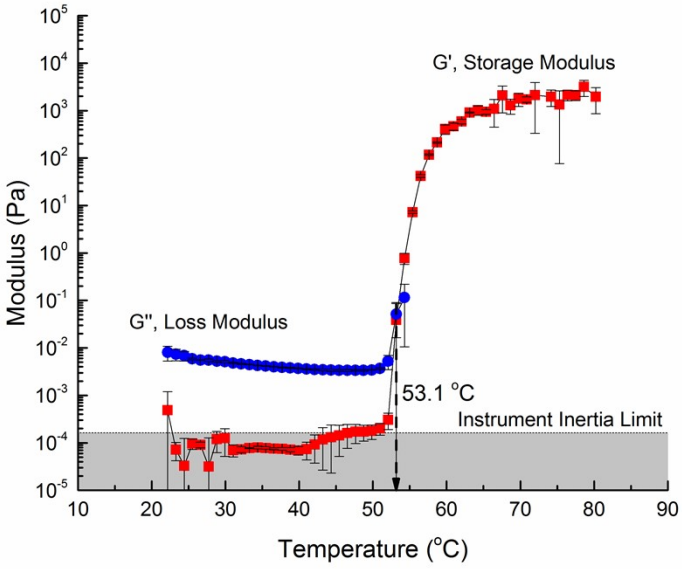

Figure S4. G' and G'' from SAOS measurements for MC 3.12 wt% (oscillation frequency = 0.1 rad/s, stress amplitude = 0.1 Pa) while warming from 20 to 80 °C at 1 °C/min.

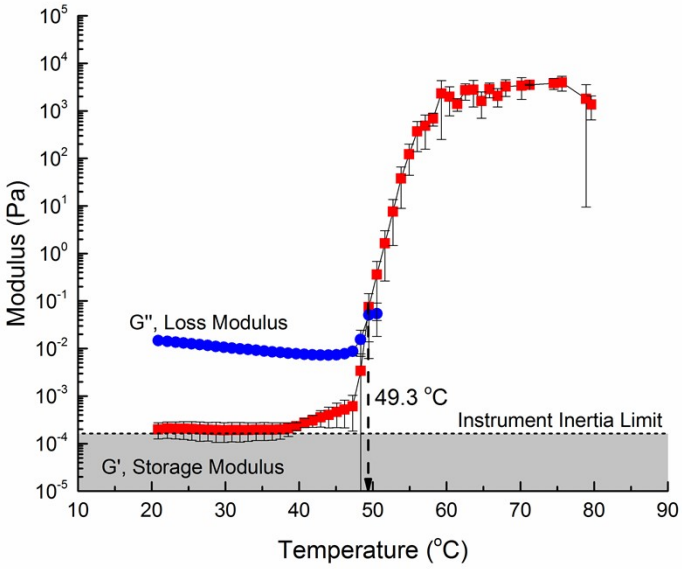

Figure S5. G' and G'' from SAOS measurements for MC 4.16 wt% (oscillation frequency = 0.1 rad/s, stress amplitude = 0.1 Pa) while warming from 20 to 80 °C at 1 °C/min.

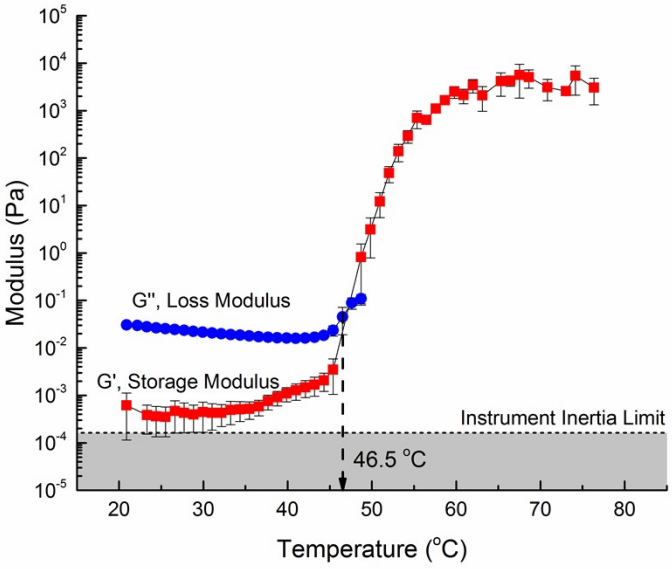

Figure S6. G' and G'' from SAOS measurements for MC 5.2 wt% (oscillation frequency = 0.1 rad/s, stress amplitude = 0.1 Pa) while warming from 20 to 80 °C at 1 °C/min.

Dynamic gel point. Figures S7 through S10 show the dynamic gelation measurements performed using the protocol detailed in the Experimental Section for all tested concentrations not shown in the main work. The “0 Pa” gel temperature denotes the quiescent gel temperature. All error bars are from three repeat measurements; error bars not shown are smaller than the data points.

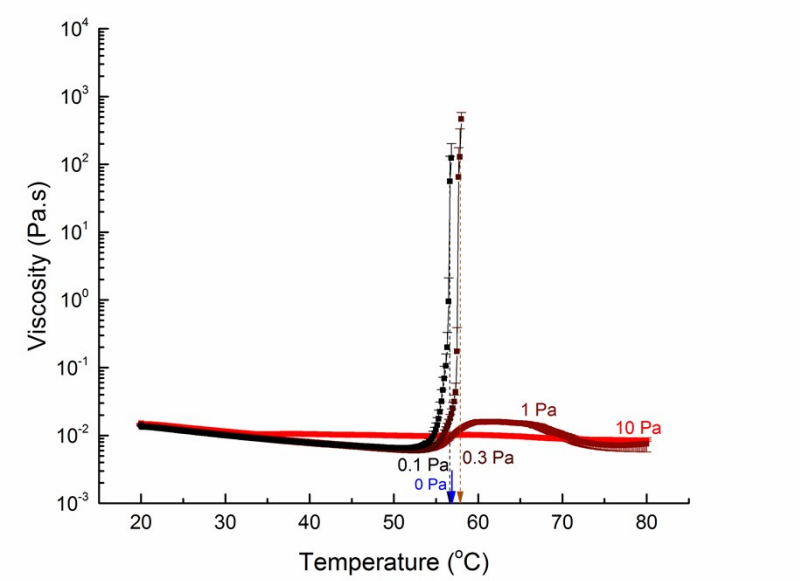

Figure S7. Growth of the steady shear viscosity for MC 2.08 wt% while warming from 20 to 80 °C at 1 °C/min while being subjected to selected shear stresses. The gelation temperatures $T_{gel}(d\eta/dT_{max})$ are marked with down-pointing arrows labeled with the applied shear stress.

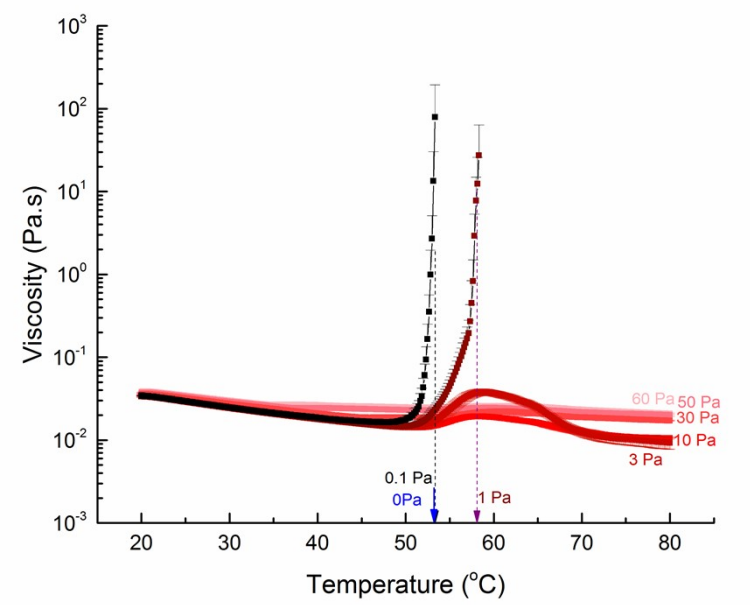

Figure S8. Growth of the steady shear viscosity for MC 3.12 wt% while warming from 20 to 80 °C at 1 °C/min while being subjected to selected shear stresses. The gelation temperatures $T_{gel}(d\eta/dT_{max})$ are marked with down-pointing arrows labeled with the applied shear stress.

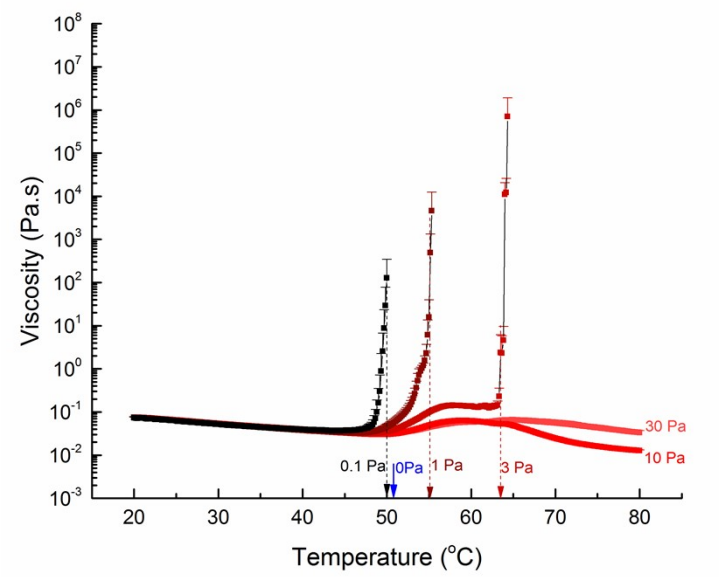

Figure S9. Growth of the steady shear viscosity for MC 4.16 wt% while warming from 20 to 80 °C at 1 °C/min while being subjected to selected shear stresses. The gelation temperatures $T_{gel}(d\eta/dT_{max})$ are marked with down-pointing arrows labeled with the applied shear stress.

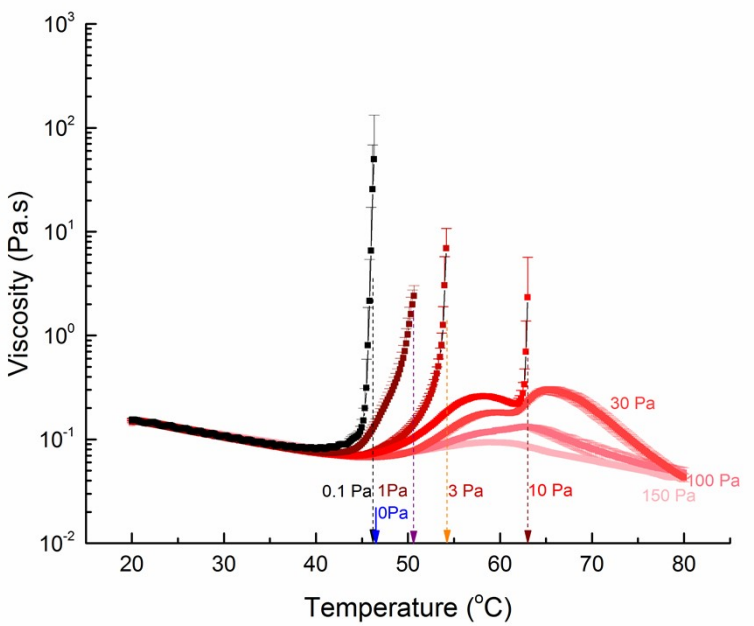

Figure S10. Growth of the steady shear viscosity for MC 5.2 wt% while warming from 20 to 80 °C at 1 °C/min while being subjected to selected shear stresses. The gelation temperatures $T_{gel}(d\eta/dT_{max})$ are marked with down-pointing arrows labeled with the applied shear stress.

Hot gel properties. Figures S11 through S14 show the hot gel storage modulus (G') obtained using the protocol detailed in the Experimental Section for all tested concentrations not shown in the main work. *G″* is omitted for clarity. In the linear viscoelastic region, *G″*/*G′* is always less than 0.1. The “0 Pa” moduli are from the “true quiescent” tests. All error bars are from three repeat measurements; error bars not shown are smaller than the data points. Data sets are truncated at first observed apparent failure.

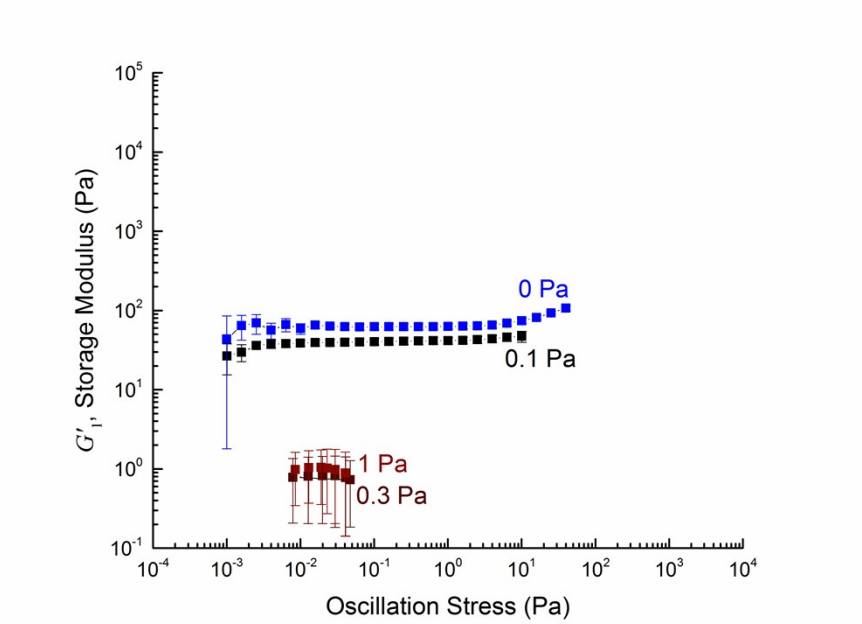

Figure S11. LAOS measurements (3 rad/s, 80 °C) for MC 1.04 wt% warmed from 20 to 80 °C at 1 °C/min while being subjected to a constant shear stress. Each stress amplitude sweep is truncated at the apparent failure stress. G'_{LVE} is obtained from a fit to the plateau at low oscillation stress.

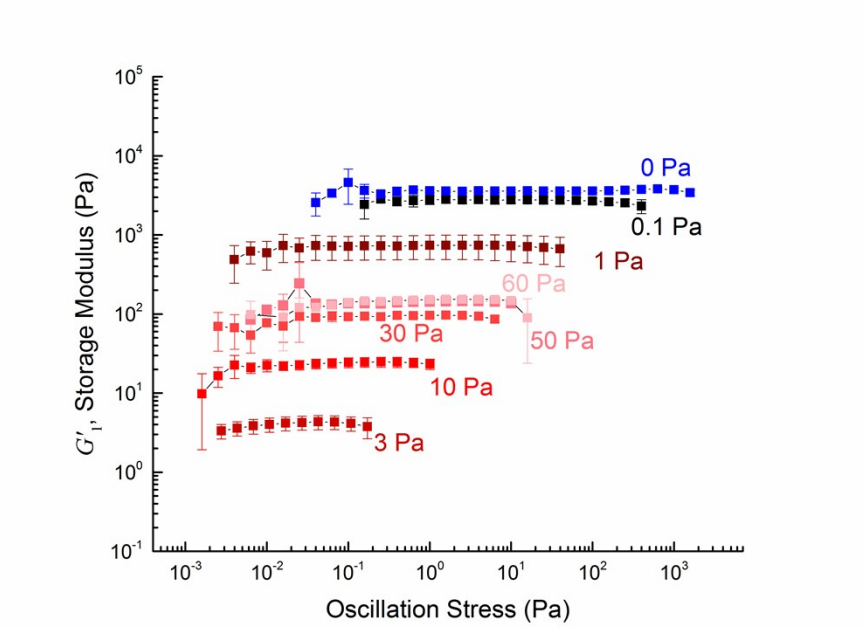

Figure S12. LAOS measurements (3 rad/s, 80 °C) for MC 3.12 wt% warmed from 20 to 80 °C at 1 °C/min while being subjected to a constant shear stress. Each stress amplitude sweep is truncated at the apparent failure stress. G'_{LVE} is obtained from a fit to the plateau at low oscillation stress.

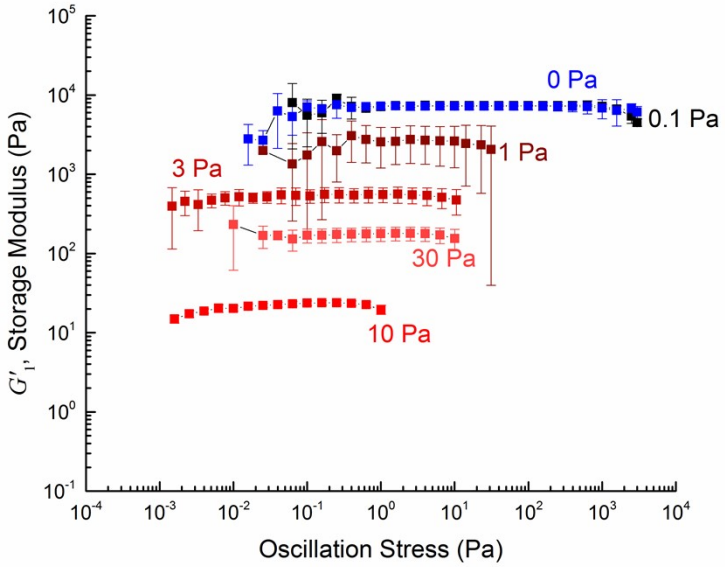

Figure S13. LAOS measurements (3 rad/s, 80 °C) for MC 4.16 wt% warmed from 20 to 80 °C at 1 °C/min while being subjected to a constant shear stress. Each stress amplitude sweep is truncated at the apparent failure stress. G'_{LVE} is obtained from a fit to the plateau at low oscillation stress.

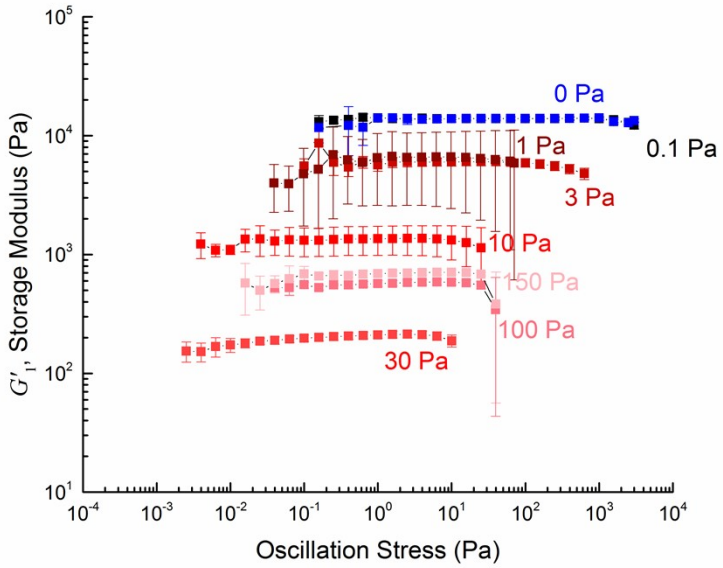

Figure S14. LAOS measurements (3 rad/s, 80 °C) for MC 5.2 wt% warmed from 20 to 80 °C at 1 °C/min while being subjected to a constant shear stress. Each stress amplitude sweep is truncated at the apparent failure stress. G'_{LVE} is obtained from a fit to the plateau at low oscillation stress.